Birefringent device converts a standard scanning microscope into a STED microscope that also maps molecular orientation

Matthias Reuss,[1,2] Johann Engelhardt,[1,2] and Stefan W. Hell[1,2,3*]

[1] *German Cancer Research Center (DKFZ), Optical Nanoscopy Division, Im Neuenheimer Feld 280, 69120 Heidelberg, Germany*

[2] *Bioquant Center, Im Neuenheimer Feld 267, 69120 Heidelberg, Germany*

[3] *Max Planck Institute for Biophysical Chemistry, Department of NanoBiophotonics, Am Fassberg 11, 37077 Göttingen, Germany*

**hell@nanoscopy.de*

Abstract: Stimulated emission depletion (STED) microscopy usually employs a scanning excitation beam that is superimposed by a donut-shaped STED beam for keeping the fluorophores at the periphery of the excitation spot dark. Here, we introduce a simple birefringent device that produces a donut-shaped focal spot with suitable polarization for STED, while leaving the excitation spot virtually intact. The device instantly converts a scanning (confocal) microscope with a co-aligned STED beam into a full-blown STED microscope. The donut can be adapted to reveal, through the resulting fluorescence image, the orientation of fluorophores in the sample, thus directly providing subdiffraction resolution images of molecular orientation.

OCIS codes: (350.5730) Resolution; (180.2520) Fluorescence microscopy; (000.2170) Equipment and techniques; (080.4865) Optical vortices;

References and Links

1. S. W. Hell, and J. Wichmann, "Breaking the diffraction resolution limit by stimulated emission: stimulated-emission-depletion fluorescence microscopy," Opt. Lett. **19**(11), 780–782 (1994).
2. T. A. Klar, S. Jakobs, M. Dyba, A. Egner, and S. W. Hell, "Fluorescence microscopy with diffraction resolution barrier broken by stimulated emission," Proc. Natl. Acad. Sci. U.S.A. **97**(15), 8206–8210 (2000).
3. E. Betzig, G. H. Patterson, R. Sougrat, O. W. Lindwasser, S. Olenych, J. S. Bonifacino, M. W. Davidson, J. Lippincott-Schwartz, and H. F. Hess, "Imaging intracellular fluorescent proteins at nanometer resolution," Science **313**(5793), 1642–1645 (2006).
4. M. J. Rust, M. Bates, and X. W. Zhuang, "Sub-diffraction-limit imaging by stochastic optical reconstruction microscopy (STORM)," Nat. Methods **3**(10), 793–795 (2006).
5. M. G. L. Gustafsson, "Surpassing the lateral resolution limit by a factor of two using structured illumination microscopy," J. Microsc. **198**(Pt 2), 82–87 (2000).
6. G. Donnert, J. Keller, R. Medda, M. A. Andrei, S. O. Rizzoli, R. Lührmann, R. Jahn, C. Eggeling, and S. W. Hell, "Macromolecular-scale resolution in biological fluorescence microscopy," Proc. Natl. Acad. Sci. U.S.A. **103**(31), 11440–11445 (2006).
7. V. Westphal, and S. W. Hell, "Nanoscale resolution in the focal plane of an optical microscope," Phys. Rev. Lett. **94**(14), 143903 (2005).
8. E. Rittweger, K. Y. Han, S. E. Irvine, C. Eggeling, and S. W. Hell, "Sted microscopy reveals crystal colour centres with nanometric resolution," Nat. Photonics **3**(3), 144–147 (2009).
9. D. Wildanger, R. Medda, L. Kastrup, and S. W. Hell, "A compact STED microscope providing 3D nanoscale resolution," J. Microsc. **236**(1), 35–43 (2009).
10. S. W. Hell, "Far-field optical nanoscopy," Science **316**(5828), 1153–1158 (2007).
11. J. Keller, A. Schönle, and S. W. Hell, "Efficient fluorescence inhibition patterns for RESOLFT microscopy," Opt. Express **15**(6), 3361–3371 (2007).
12. B. Harke, J. Keller, C. K. Ullal, V. Westphal, A. Schönle, and S. W. Hell, "Resolution scaling in STED microscopy," Opt. Express **16**(6), 4154–4162 (2008).
13. D. Wildanger, E. Rittweger, L. Kastrup, and S. W. Hell, "STED microscopy with a supercontinuum laser source," Opt. Express **16**(13), 9614–9621 (2008).
14. N. Bokor, Y. Iketaki, T. Watanabe, and M. Fujii, "Compact fluorescence depletion microscope system using an integrated optical element," Opt. Commun. **281**(7), 1850–1854 (2008).

#119893 - $15.00 USD Received 12 Nov 2009; revised 28 Dec 2009; accepted 28 Dec 2009; published 7 Jan 2010

15. R. Menon, P. Rogge, and H.-Y. Tsai, "Design of diffractive lenses that generate optical nulls without phase singularities," J. Opt. Soc. Am. A **26**(2), 297–304 (2009).
16. D. Wildanger, J. Bückers, V. Westphal, S. W. Hell, and L. Kastrup, "A STED microscope aligned by design," Opt. Express **17**(18), 16100–16110 (2009).
17. G. Machavariani, Y. Lumer, I. Moshe, A. Meir, and S. Jackel, "Efficient extracavity generation of radially and azimuthally polarized beams," Opt. Lett. **32**(11), 1468–1470 (2007).
18. M. Dyba, J. Keller, and S. W. Hell, "Phase filter enhanced STED-4Pi fluorescence microscopy: theory and experiment," N. J. Phys. **7**, 134 (2005).
19. N. Bokor, Y. Iketaki, T. Watanabe, K. Daigoku, N. Davidson, and M. Fujii, "On polarization effects in fluorescence depletion microscopy," Opt. Commun. **272**(1), 263–268 (2007).
20. V. Westphal, C. M. Blanca, M. Dyba, L. Kastrup, and S. W. Hell, "Laser-diode-stimulated emission depletion microscopy," Appl. Phys. Lett. **82**(18), 3125–3127 (2003).
21. P. Török, and P. Munro, "The use of Gauss-Laguerre vector beams in STED microscopy," Opt. Express **12**(15), 3605–3617 (2004).
22. I. Testa, A. Schönle, C. von Middendorff, C. Geisler, R. Medda, C. A. Wurm, A. C. Stiel, S. Jakobs, M. Bossi, C. Eggeling, S. W. Hell, and A. Egner, "Nanoscale separation of molecular species based on their rotational mobility," Opt. Express **16**(25), 21093–21104 (2008).
23. M. A. Lieb, J. M. Zavislan, and L. Novotny, "Single-molecule orientations determined by direct emission pattern imaging," J. Opt. Soc. Am. B **21**(6), 1210–1215 (2004).
24. M. Böhmer, and J. Enderlein, "Orientation imaging of single molecules by wide-field epifluorescence microscopy," Opt. Soc. Am. B **20**(3), 554–559 (2003).
25. P. Dedecker, B. Muls, J. Hofkens, J. Enderlein, and J. I. Hotta, "Orientational effects in the excitation and de-excitation of single molecules interacting with donut-mode laser beams," Opt. Express **15**(6), 3372–3383 (2007).
26. D. Patra, I. Gregor, and J. Enderlein, "Image Analysis of Defocused Single-Molecule Images for Three-Dimensional Molecule Orientation Studies," J. Phys. Chem. A **108**(33), 6836 (2004).
27. T. Ha, T. Enderle, S. Chemla, R. Selvin, and S. Weiss, "Single molecule dynamics studied by polarization modulation," Phys. Rev. Lett. **77**(19), 3979–3982 (1996).
28. B. Sick, B. Hecht, and L. Novotny, "Orientational imaging of single molecules by annular illumination," Phys. Rev. Lett. **85**(21), 4482–4485 (2000).

1. Introduction

Fluorescence microscopy is one of the most extensively used tools for the structural and functional investigation of the interior of cells. Its popularity has steadily grown despite the fact that it notoriously fails to image structures smaller than about half the wavelength of light (~200 nm). While electron, X-ray, and scanning probe microscopy offer a substantially better resolution, they all fall short in imaging intact or even living cells in three dimensions (3D).

The invention of Stimulated Emission Depletion Microscopy (STED) in 1994 highlighted the then unexpected fact that the diffraction resolution barrier can be effectively overcome in a microscope that uses regular lenses and focused visible light [1,2]. Other subdiffraction resolution techniques, such as PALM, STORM and structured illumination have since emerged as well [3–5]. STED microscopy currently provides nanometer scale resolution [6–8] in biological and non-biological samples, while retaining most of the advantages of far-field optical operation, such as the ability to non-invasively image cells in 3D [9].

While the principles of scanning STED microscopy do not rest on those of the confocal microscope, STED can be implemented in a scanning confocal microscope to great effect. To this end, one overlaps the focused excitation beam of a scanning (confocal) microscope with a donut-shaped STED beam [10,11], whose role is to keep fluorophores dark even when they are exposed to excitation photons. The fluorophores remain dark, because the wavelength and the intensity of the STED beam are adjusted such as to instantly de-excite potentially excited fluorophores by stimulated emission. Consequently, fluorophores subject to a STED beam of intensity $I > 3\, I_s$ are practically confined to the ground state and hence switched off. This is a consequence of the fact that the normalized probability of the molecule to spend time in the excited state follows $\sim \exp(-I/I_S)$, with I_s being a characteristic of the molecule. Any molecule subject to $I >> I_s$ is deprived of its ability to fluoresce, because the fluorescent state is disallowed by the presence of the STED beam. Since I increases from the center of the donut on outwards to the donut crest, the probability for a molecule to be off is highest at the donut crest. Molecules located at the donut center remain fluorescent. At a certain distance from the center where $I > 3\, I_s$, practically all molecules (95%) will be off. Since the threshold

#119893 - $15.00 USD Received 12 Nov 2009; revised 28 Dec 2009; accepted 28 Dec 2009; published 7 Jan 2010

$3\,I_s$ can be moved towards the center by increasing the overall intensity of the STED-beam, the region in which the fluorophores are still capable of signaling can be decreased far below the physical width of the donut minimum, i.e. far below the diffraction barrier.

Specifically, for a wavelength λ and a numerical aperture NA of the objective lens, the spot in which the fluorophores are able to signal will have a diameter $d \approx \lambda/(2\,NA\sqrt{1+I_m/I_s})$ [7,12]. I_m is the intensity of the STED-beam at the donut crest. I_s is usually on the order of 1-10 MW/cm^2. Scanning the two overlapped beam reveals structures at a resolution d, because the signal of fluorophores that are further apart than *d* are recorded sequentially in time. With several current dyes, *d* can thus be shrunk down to ~20 nm [6,7]; for a certain class of inorganic fluorophores (crystal color centers) even 5.8 nm have been reported [8].

An important point in setting up and operating a STED microscope is beam alignment. For maximum performance, the donut should be centered on the excitation spot with deviation < 50 nm. Furthermore, the beam alignment should be stable over the course of a measurement and over an adequate field of view. While this is in not an obstacle in principle, given that in standard multi-color confocal microscopes several beams are superimposed with a comparable precision, too, it is desirable to improve stability and ease of operation by having pre-aligned beams.

Intrinsic alignment can be achieved by using a common laser source for both the excitation and the depletion beam. This can be accomplished by coupling two separate lasers into a common optical fiber or, even more conveniently, by using a super-continuum light source [13]. However, having pre-aligned beams requires a beam shaping device that leaves the excitation wavelength unaffected, while treating the STED wavelength in such a way that it forms a donut. Current donut-shaping devices however use a vortex phase mask and cannot sufficiently distinguish between wavelengths. They also forge the excitation beam into something close to a donut and are thus not suitable for the use with pre-combined beams. The solution suggested in [14] relies on the annular separation of pre-aligned beams but blocks a considerable amount of STED light. The method proposed in [15] has, up our knowledge, not been realized in practice so far. More recently, Wildanger et al. [16] proposed a scheme that relies on the different dispersion properties of different optical materials. By selecting two optical glasses whose refractive indices match at the excitation wavelength but differ for the STED wavelength, they were able to design a phase plate that can be shared by both beams. In their scheme, however, the detection beam path is coupled out between the objective lens and the phase plate using a dichroic mirror.

Here we introduce a beam shaping device that stands out by the fact that it is placed directly in front of the objective lens. Contrary to the previous methods, it does not rely on introducing phase differences, but rather on modifying the polarization across the cross-section of the STED beam. Working with polarization, one can advantageously use birefringent crystals which are commercially available in high quality as low order optical retarders. The typical chromatic characteristics of a low order waveplate exactly match the spectral separation of the excitation and the STED-beam. Thus, we have built a simple, error-proof and easy-to-use beam-shaping device that, together with an appropriate laser source, can economically retrofit almost any standard scanning (confocal) fluorescence microscope and turn it into a full STED microscope (easySTED) providing subdiffraction resolution.

Furthermore, with a minor change, the same beam shaping device can be tuned so that the image of a single fluorophore depends strongly on the fluorophore's transition dipole orientation. As a result, this *M*olecular *O*rientation *M*icroscopy by STED (MOM-STED) allows one to assess the orientation of the transition dipole of the molecule in space. Most intriguingly, the orientation of the molecule is directly reproduced in the image by a (line-shaped) fluorescence patch. In addition, by sensing subtle changes in molecular orientation, this simple yet powerful version of STED microscopy improves the recognition and hence separation of adjacent individual fluorophores. By the same token, MOM-STED also allows one to improve counting of molecules within subdiffraction sample volumes.

#119893 - $15.00 USD Received 12 Nov 2009; revised 28 Dec 2009; accepted 28 Dec 2009; published 7 Jan 2010

2. Design of the beam shaping device

The central part of our beam shaping device consists of a segmented low-order wave plate with the fast axes oriented as shown in Fig. 1. The four segments were cut from a single

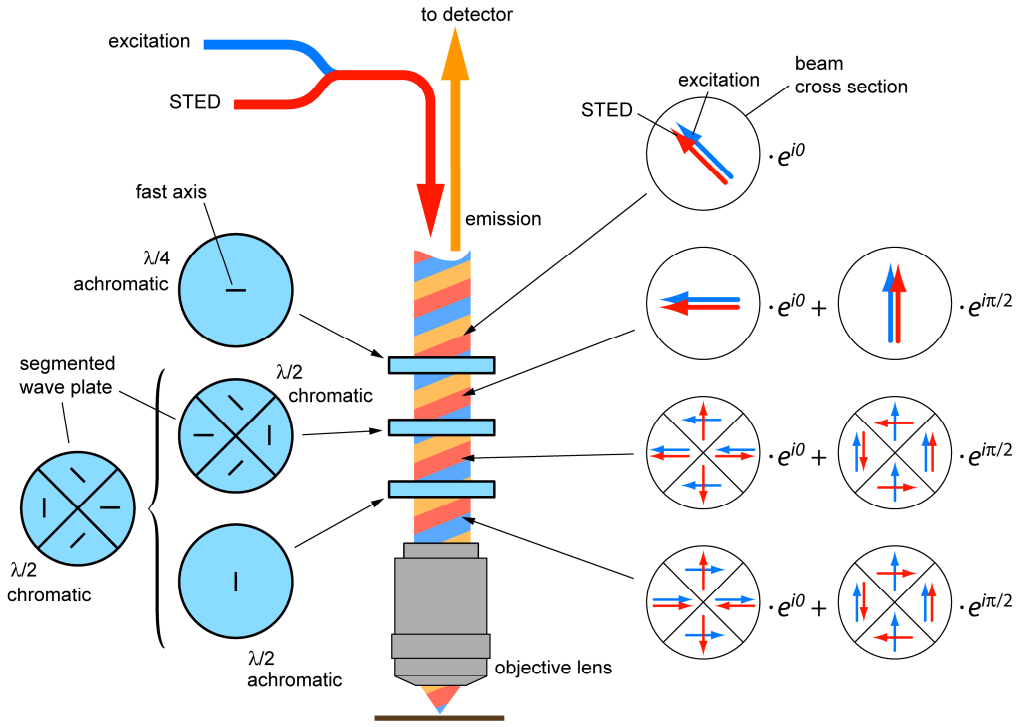

Fig. 1. Schematic setup of an easySTED microscope using a birefringent beam shaping device directly in the back of the objective lens. *Center:* principle beam path. Excitation (blue)- and STED-beams (red), as well as emitted fluorescence light (yellow) pass the beam shaping device. Preferably, STED and excitation light are provided by the same source to facilitate intrinsic beam alignment. *Left side:* Schematic drawing of the beam shaping device, consisting of three wave plates, where the last two wave plates can be combined into a single segmented one, as indicated. *Right:* polarization state of the excitation- and STED-beams at different stages in the beam shaping device and at two representative points of the wave cycle. The two beams are treated differently due to the chromatic nature of the segmented wave plate. The STED beam will focus to a donut, whereas the excitation beam leaves the device circularly polarized, rendering a normally focused light spot.

bigger wave plate in order to ensure a constant overall thickness. Subsequently, the four segments were put together again by cementing them onto a common substrate (BK7), while observing the proper orientation of the fast axis. The orientation of the fast axes is similar to the orientation suggested in [17] for generating an azimuthally polarized beam; the only difference is the number of segments. Two devices were manufactured, one for performing STED at 647 nm (line from an argon-krypton laser) and one for STED at 592 nm (rendered by a frequency-doubled fiber laser). The utilized excitation wavelengths are 532 nm and 504 nm, respectively. In both cases, the retardation of the respective wave plate is 2.5λ for the STED line and $\sim 3\lambda$ for the excitation line. As a result, the STED line experiences a half-wave retardation leading to a rotation of the polarization plane, whereas the excitation beam is unaffected. In combination with an achromatic half wave plate, we achieve donut focusing for the STED wavelength, while the excitation beam is focused to a regular nearly diffraction-limited focal spot.

#119893 - $15.00 USD Received 12 Nov 2009; revised 28 Dec 2009; accepted 28 Dec 2009; published 7 Jan 2010

Additionally, an achromatic quarter wave plate ensures that all molecules are effectively excited and quenched, regardless of their orientation (easySTED). Provided that only the segmented wave plate is employed and the two achromatic retarders are left out, the depletion process becomes sensitive to molecular orientation and the direction of molecular dipoles can be investigated. This way, with a simple conversion, the beam shaping device can be used both for isotropic resolution enhancement and for directionality assays. If the latter is not desired, the segmented wave plate and the plain half wave plate can be combined into a single segmented half wave plate.

The right hand side of Fig. 1 depicts the polarization direction of the STED and the excitation beams at several positions in the beam shaping device and at two different points of the wave cycle. First, both linearly polarized beams are circularly polarized by the achromatic quarter wave plate. Then, the polarization is selectively rotated for the STED beam only by the segmented wave plate. At this stage, the STED beam is radially polarized for phases $\phi = 0$ and azimuthally polarized for $\phi = \pi/2$, with both polarization states being unfavorable for STED microscopy. The final $\lambda/2$ retarder selectively flips the horizontally polarized components of both beams, reversing the circular polarization of the excitation beam and turning the STED beam into a donut for all points of the wave cycle.

Figure 2a shows the electric field of the STED donut in the focal plane. While for $\phi = 0$, the intensity distribution is ring-like with a central zero (indicating good STED performance), the field distribution causes the effective excited state depletion pattern to depend on the orientation of the fluorophore about to be quenched. In our example, the state of the molecule oriented at 45° will be depleted most effectively by the upper left and by the lower right portion of the STED-beam where the electric field is parallel to the transition dipole. In contrast, the regions where the E-field is polarized perpendicularly do not act on the molecule. This leads to high resolution only in regions to the left and to the right of the dipole. However, with $\phi = \pi/2$, resulting from the action of the first quarter wave plate, the polarization is rotated by 90° and the resolution is enhanced in a direction parallel to the dipole orientation. Thus, when averaging over many cycles, one obtains high optical resolution in all directions.

Note that the electric field distribution shown in Fig. 2a is in principle the same as in a donut created using a vortex phase element that has become the quasi-standard for STED microscopy. In addition, our beam shaping device allows the incoming STED light to be both left and right circularly polarized after the first achromatic quarter wave plate as can be seen when tracing the right side of Fig. 1 with different orientation of the polarization. This is an important point, as it allows one to easily combine two STED-sources via a polarizing beam splitter in order to double the available STED power. Standard vortex phase plates and the phase plate described in [16] cannot forge both the resulting polarization directions into a donut; instead the STED beam path will have to be split up again with all the

#119893 - $15.00 USD Received 12 Nov 2009; revised 28 Dec 2009; accepted 28 Dec 2009; published 7 Jan 2010

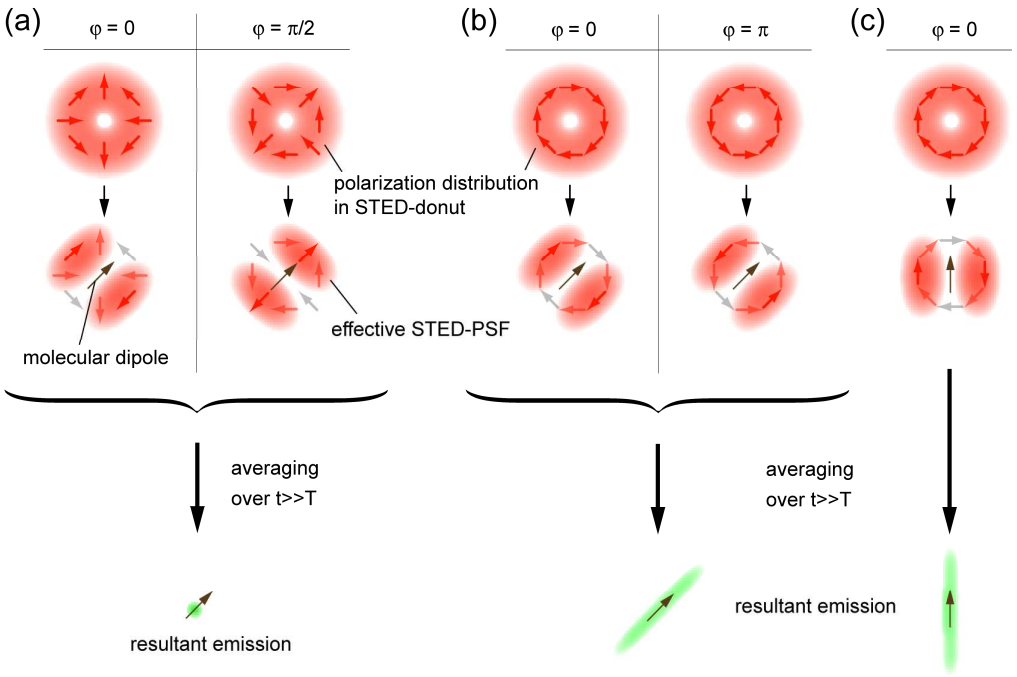

Fig. 2. Effect of the STED beam on a fluorescent molecule with easySTED *(a)*, and with Molecular Orientation STED Microscopy (MOM-STED) *(b, c)*. *(a):* Polarization distribution in the STED-donut for phases 0 and $\pi/2$ *(top row)*, and the resultant effective STED beam focal spot (STED-PSF) in the *second row,* taking into account the projection of the STED-field onto the dipole. The effective STED PSFs for $\phi = 0$ and $\phi = \pi/2$ complement each other and lead to high resolution in all directions. *(b):* with MOM-STED, the resulting effective STED PSF is the same for all ϕ and resolution enhancement is parallel to the dipole only. In *(c)*, a molecule with different orientation is shown; also in this case, the molecule is subject to the STED field only in those regions where the STED-field is parallel to the dipole. It can be seen that with MOM-STED this is always the case in a direction perpendicular to the dipole, regardless of its actual orientation.

negative effects on beam alignment. In contrast, the segmented wave plate generates a donut regardless of the incoming polarization.

At first sight, the polarization pattern for a donut shown in Figs. 1 and 2a appears unnecessarily complex. It seems much simpler to employ an azimuthally polarized beam as suggested in [17], because azimuthal polarization in the back focal plane will transform into a focal intensity distribution with a central minimum. In practice, however, this distribution of the electric field in the focal plane is unfavorable for STED, because the transition to the ground state, i.e. the depletion of the excited state of an azimuthally polarized donut depends on the orientation of the fluorescent molecules [18–21]. On the other hand, this means that such a donut is of great use when it comes to finding out the actual direction of molecular dipoles.

In fact, by leaving out the two plain non-segmented wave plates in Fig. 1, STED becomes sensitive to molecular orientation. The resulting distribution of the electric field in the focal plane is discussed in Fig. 2b,c together with the effect on the detection PSF. Every molecule is quenched only in a direction perpendicular to its dipole. In directions along the dipole, regardless of its actual orientation, the STED-field has no component parallel to the dipole and thus cannot elicit a molecular transition, i.e. not effect the exited state depletion. In contrast to Fig. 2a, the parts of the donut where the molecule cannot be depleted are the same for all phases. Hence, the resulting resolution enhancement is not isotropic and this device can

#119893 - $15.00 USD Received 12 Nov 2009; revised 28 Dec 2009; accepted 28 Dec 2009; published 7 Jan 2010

be used to investigate the orientation of fluorescent molecules in a sample, provided that the dipoles are rotationally immobile. We have thus created a microscope for directly mapping the molecular orientation.

4. Experiments

Figure 3 shows the STED-PSF (red) and the excitation-PSF (blue) in an overlay in the focal plane and as line profiles. The images were obtained by scanning a 80 nm gold bead through the focal region (BBInternational, UK, prepared similary to the fluorescent bead sample in [12]). Evidently, the STED beam is forged into a donut, while the excitation is a plain focal spot, as expected. The STED-PSF has a slight four-leafed appearance which is due to the four pieces of the segmented wave plate. The modulation along the donut crest is < 20% and has no practical impact on the STED performance, as is discussed below.

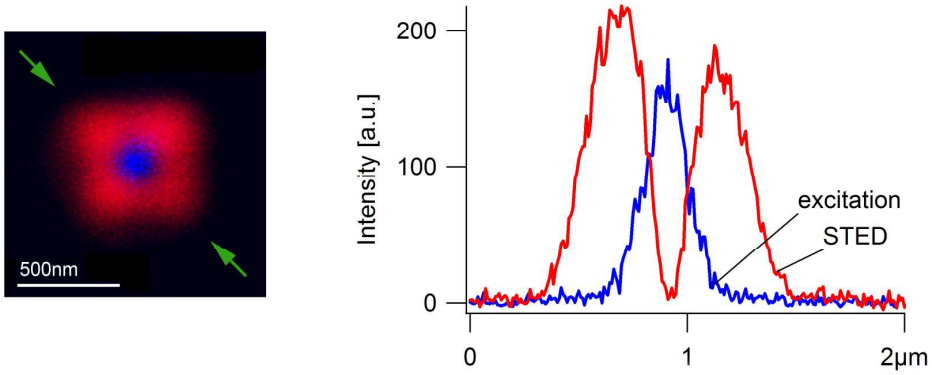

Fig. 3. Beam shaping with a segmented waveplate device. *Left:* focal intensity distributions of the excitation (blue) and STED (red) beam. Both beams have passed the easySTED beam shaping device simultaneously. The 647nm-STED beam becomes a donut, while the 532nm-excitation beam is focused to a regular spot. *Right:* line profiles along the direction indicated by the arrows on the left.

In Fig. 4, fluorescent beads stained with the fluorophore nile red (20nm FluoroSpheres, Invitrogen, USA, sample preparation as in [12]) have been imaged both in standard confocal mode and with easySTED. The excitation wavelength was 532 nm, the STED beam was a modelocked 647 nm Ar/Kr beam (80MHz repetition rate, ~200ps pulse duration) with an

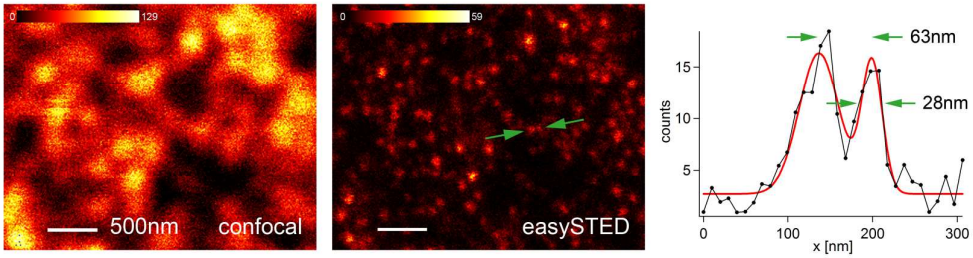

Fig. 4. Resolution enhancement with easySTED. Fluorescent beads imaged in standard confocal mode *(left)* and with high-resolution easySTED *(center).* The plot framed green *(right)* shows a line profile (black) along the arrows indicated in the central easySTED image together with a double Gaussian fit (red). Scale bar = 500 nm; count rates are in counts/200µs dwell time.

intensity of ~200MW/cm^2 in the focal plane. The resolution enhancement provided by STED is obvious; the smallest features in the image indicate a resolution of ~30 nm, as can be

#119893 - $15.00 USD Received 12 Nov 2009; revised 28 Dec 2009; accepted 28 Dec 2009; published 7 Jan 2010

inferred from a Gaussian fit to a line profile (see Fig. 4, right). The resolution is most likely limited by the available STED power. Most noteworthy, the resolution we obtain with a standard vortex phase plate on otherwise the same setup and the same sample is also in the 30nm range. Furthermore, no asymmetries in the effective PSF are noticeable that might be expected due to the fact that the STED-PSF is not a pure donut mode (see Fig. 3). Altogether, this shows that the technical simplifications behind easySTED actually do not come at the cost of performance.

The fluorescence emission, whose maximum is close to the excitation line, is mostly left unaffected by the beam shaping device too, otherwise the signal would drop considerably at the confocal detection pinhole. Importantly, this allows the device to be installed directly behind the objective lens in the first place. Note that the confocal pinhole is needed only if 3D sectioning is required; the STED principle does not require confocality because the region from where the fluorescence originates is predefined by the position of the minimum of the STED beam.

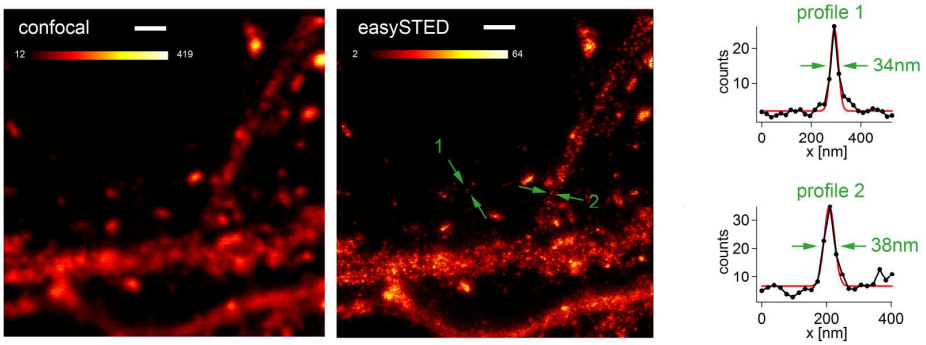

Fig. 5. EasySTED on biological samples. The protein *bassoon* in hippocampal mouse neurons observed in standard confocal mode *(left).* In contrast, easySTED (*center*) reveals detail unobservable in the confocal image. Both images show raw data. *Right:* profiles along the lines indicated by arrows in the easySTED image together with Gaussian fits reveal a resolution below 40nm. Scale bars are 1µm, count rates are in counts/200µs dwell time.

Figure 5 shows images taken from hippocampal mouse neurons in standard confocal mode and with STED using our polarization beam shaping device. The presynaptic active zone protein *bassoon* was labeled with A565 dye (Atto-Tec, Germany). Beam parameters were the same as in Fig. 4. Again, easySTED reduces the area of the effective focal spot by a factor of ~40. For the easySTED image, the apparent size of unspecifically bound single antibodies indicates a lateral resolution of the STED microscope of around 35 nm. The average size of the protein features is 80 nm. Thus, the actual distribution of the protein *bassoon* and the shape of the active zone can be fully assessed.

Figure 6 shows MOM-STED as discussed in Fig. 2b, c. Single nile red molecules have been prepared by using the bead sample from above and bleaching an area with the excitation laser until a sufficiently low number of dye molecules were left in the beads. Thus, we obtain individual molecules surrounded and fixed in orientation by polystyrene, which we have found to be advantageous in terms of brightness and photostability. Furthermore, these beads provide us with a well-defined environment for the first demonstration of MOM. This sample was then imaged confocally and with STED using pure azimuthal polarization. The resulting molecular images depend on the orientation of their transition dipoles. To further reduce the number of visible molecules, we used linearly polarized excitation (vertically in Fig. 6) by exciting only molecules with a vertical dipole component. This explains the preferential orientation of the molecules in Fig. 6. When the polarization of the excitation beam is rotated, the dominant direction of the apparent molecules will rotate as well.

The magnification in the green box shows what, most likely, is a single molecule that has been resolved down to 40 nm perpendicular to its dipole direction; yet it has the 180 nm-width

#119893 - $15.00 USD Received 12 Nov 2009; revised 28 Dec 2009; accepted 28 Dec 2009; published 7 Jan 2010

of a standard confocal spot image along the dipole. From this asymmetric image, the orientation of the dipole in the focal plane can be inferred.

Furthermore, the ability to discern molecules which differ in their orientation means they could be individually imaged and counted even when their intermolecular distance is only a few nanometers or below. Assessing the orientation of molecules that are separated by a sub-diffraction distance has so far been mostly impossible with current techniques, because they rely on the polarization of the emitted light. In contrast, operating with the polarization of illumination, MOM opens up an additional parameter for separation. The green arrow in Fig. 6 shows a situation where the molecules are so close together that most likely they could not have been resolved with an isotropic resolution of 40 nm. In contrast, MOM allows their differentiation due to clearly distinct image shapes. One could go as far as to fit with several elongated and appropriately rotated images in order to find the exact location of the emitters.

As for biological specimens, there is considerable evidence [22] that they do indeed contain at least a fraction of fixed molecules, for example in fully assembled actin filaments and bundles, indicating that imaging the molecular orientation should become important.

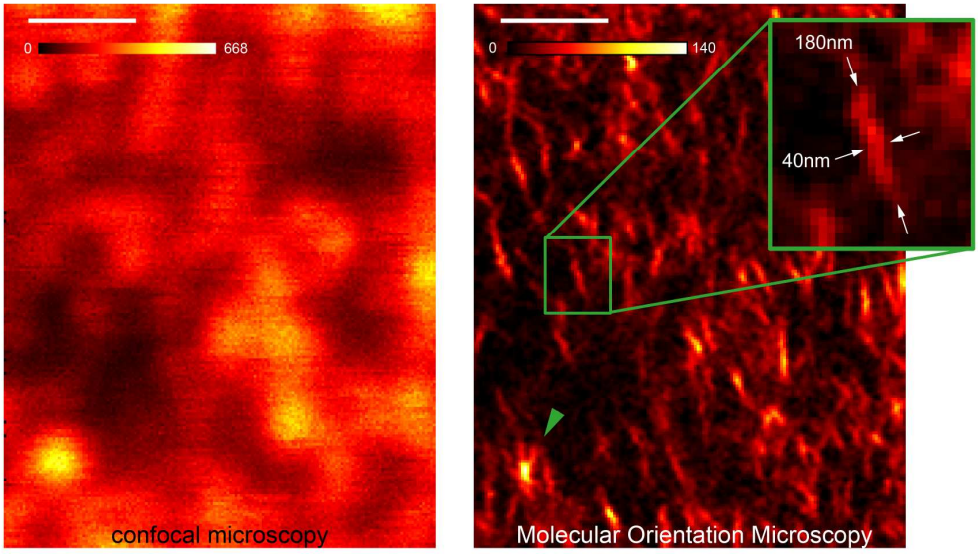

Fig. 6. Molecular Orientation Microscopy (MOM) by STED on nile red fluorescent beads bleached down to almost single molecule level. The resolution with STED is enhanced only in directions perpendicular to the dipole of the molecule, as is evident from the magnification on the right. The molecules being mostly vertically aligned is a result of the linearly polarized excitation beam that preferably acts on molecular transition dipoles along this direction. Green arrow: three molecules can be separated even in a sub-STED focal volume solely by the fact that their resulting spot differs in orientation. Scale bars are 500nm, count rates are in counts/1000µs dwell time.

5. Conclusions

We have designed a wavelength-sensitive beam shaping device for easySTED microscopy. Because it has a different effect on the excitation-, emission- and the STED-beams, all beams can simultaneously pass the device. This facilitates intrinsic alignment when a common source is employed for excitation and for STED or when both beams are fed through the same optical fiber. This way, it consequently simplifies the assembly, maintenance, and operation of a STED microscope.

The beam shaping device itself consists mainly of a segmented half wave plate that can be easily manufactured from an off-the-shelf retarder in two steps using standard procedures. Straightforward and robust in production as well as in operation, our beam shaping device can

#119893 - $15.00 USD Received 12 Nov 2009; revised 28 Dec 2009; accepted 28 Dec 2009; published 7 Jan 2010

be used to retrofit standard scanning fluorescence (confocal) microscope by placing the device behind the objective lens and adding a laser that delivers the STED-beam. Moreover, our work clearly indicates that a specific STED objective lens could be manufactured with a segmented wave plate already incorporated, similar to lenses for phase contrast microscopy.

Additionally, with a minor change, our device can be used for investigations on the orientation of fluorescent molecules. Reported methods for determining the orientation mostly rely on comparing the (rather complicated) defocused diffraction pattern to theoretical predictions and/or on special illumination/detection schemes [23–26] [27,28], for instance annular illumination. In any case, these methods demand a good signal-to-noise ratio and are a rather indirect. In contrast, MOM sorts out the molecular orientation directly in the sample and the orientation in the focal plane can be seen immediately from the image. A future application of MOM could be in the field of molecular motors. While much is known about their linear stepping, MOM would also allow one to find out about how the motor twists as it moves along its track.

Note that STED *per se* is, of course, not essential to this way of establishing molecular orientation. In fact, any saturable optical transition between two states can be used to establish molecular orientation in this way [10]. In other words, MOM using STED can be readily expanded to a MOM-RESOLFT concept where stimulated emission is replaced by an electron spin flip (triplet state transition) or the relocation of atoms such as a cis-trans photoisomerization, a reversible formation of chemical bonds, etc [10]. Clearly the same donuts and related versions thereof can be utilized in the RESOLFT approach. The importance of creating local minima in nanoscopy concepts based on separating features by coordinate-targeted switching (RESOLFT) underscores the importance of the birefringent elements and the specific minima reported herein [10]. Moreover, even if the spatial resolution does not suffice to resolve the molecules in space, as long as their dipole orientation differs, molecules can be separated and counted in a volume with high sensitivity.

Acknowledgements

We thank T. Dresbach from Heidelberg University for preparing the samples in Fig. 4, G. Zinner from B. Halle for qualified support, T. Staudt for valuable discussions and J. Jethwa for critical reading. M. R. acknowledges a doctoral fellowship from the DKFZ. This work was supported through the Gottfried-Wilhelm-Leibniz prize of the Deutsche Forschungsgemeinschaft (to S.W.H.).

#119893 - $15.00 USD Received 12 Nov 2009; revised 28 Dec 2009; accepted 28 Dec 2009; published 7 Jan 2010